Plasmonic D-Shaped Photonic Crystal Fiber Biosensor with Gold Layer for Sensing of the Refractive Index

Mir Vahid Kazempour* and Hamid Vahed

Faculty of Electrical and Computer Engineering, University of Tabriz, Tabriz, Iran

***Corresponding author Email:** vahid.kazempour@yahoo.com

Regular paper: Received: Jan. 10, 2021, Revised: Mar. 7, 2021, Accepted: May. 15, 2021, Available Online: May. 17, 2021, DOI: 10.29252/ijop.14.2.209

ABSTRACT— In this paper, we propose a D-shaped plasmonic optical biosensor based on photonic crystal fiber (PCF) to detecting of the different materials such as water, blood plasma, Yd-10B and hemoglobin by using of the refractive index. The gold layer is coated on the polished surface of D-shaped fiber. To achieve the highest sensitivity of the proposed biosensor, we investigated the effects of variation of the gold layer thickness and the other structure parameters such as hole diameter (d) and the distance between two holes or Pitch (Λ). The results show that the most sensitivity of the proposed biosensor is 2506 nm per refractive index unit (nm/RIU) with the resolution of 1.25×10^{-5} RIU, when d=1.4 μm and Λ=1.9 μm with the gold layer thickness of 45nm.

KEYWORDS: Surface Plasmon Resonance, Photonic Crystal Fiber, Biosensor, Sensitivity

I. INTRODUCTION

In recent years, Optical fiber sensors based on surface plasmon resonance (SPR) is considered in different fields such as sensing and biomedicine [1-6]. At a certain wavelength of the transverse magnetic mode (TM) which refer to the wavelength resonance, surface plasmon polariton (SPP) excited between of an electric layer (metal) and a dielectric layer (sensing layer) that leads to coupling energy between the fundamental mode of core and the sensing layer [7-8]. Moreover, the SPR optical sensors based photonic crystal fibers (PCFs) are considered as the temperature sensor, the electric field sensor and the refractive index (RI) sensor, because of its unique properties such as small size, and the high flexibility [9-12]. Also, the changing of the structural properties such as the distance between two holes (pitch), the diameter of holes (d), the material of holes, the thickness of layers, and the material of the metal layer is usual in these biosensors to enhance the performance characteristic of biosensor [13-17]. Therefore, it is possible to achieve the optimal structure with the maximum sensitivity of the designed biosensor. Recently, M.N. Sakib *et al.* numerically analyzed an SPR sensor based on dual core D-shape PCF. Their results show that the maximum wavelength sensitivity of 8000 nm per refractive index unit (nm/RIU) for sample measurement range from 1.45 RIU to 1.48 RIU [18]. H. Thenmozhi *et al.* investigated D-Shaped PCF sensor based on SPR with coating of indium titanium oxide (ITO) and achieved the maximal spectral sensitivity of 50000 nm/RIU [19]. S. Singh *et al.* studied a D-shaped PCF sensor to sense the refractive index ranging from 1.32 to 1.40 which consist of the gold and the graphene layers with relatively complicated structure of air holes [20]. W. Zeng and *et al.* proposed a SPR sensor based on D-shaped PCF for detection of the refractive index that consist of two nanoscale gold belts and asymmetric core [21]. M.B. Hossain *et al.* designed a quasi D-shaped PCF-SPR biosensor that PCF lattice was created with three air hole formed rings with one missing hole in the second circular ring to formation of the birefringence [22]. Most of the papers reviewed above contain the dual-core fiber

structures or have the complex structures with a variety of defects. Therefore, the experimental design and construction of these sensors will have experimental difficulty. But, the structure of our proposed sensor is a single-core fiber with a symmetrical and simple design that shows the advantage of structure and the experimental realization with the appropriate sensitivity. In this paper, the D-shaped SPR optical biosensor based on PCF is investigated and analyzed by using of Finite Difference Time Domain (FDTD) method from Lumerical Solutions Inc to detecting of the different materials by using of the refractive index. We studied the confinement loss spectrum of the proposed biosensor, the resonance wavelengths and the relative sensitivity. Finally,we introduced the optimal structure with the highest sensitivity.

II. MATERIALS AND METHODS FOR PROPOSED BIOSENSOR

Two dimensional (2D) basic structure of the proposed D-shaped SPR biosensor based on PCF with the hexagonal lattice is shown in Fig.1. The thickness of the gold layer is fixed with d_{Au}=45nm and it is deposited on the polished cross-section of D-shaped SPR biosensor by depth of $h = 2.6\mu m$. The lattice pitch is $\Lambda = 2\mu m$ and the diameter of the air holes is d=1.4 μm. Perfect matched layer (PML) boundary condition is set for the outermost layer boundaries of fiber. Here, the background material of the fiber is fused silica and its dispersion can be calculated by the Sellmeier equation [3-5].

In addition, the dielectric constant of the gold layer is defined by drude model which can be determined as [8-9]:

$$\varepsilon_m = \varepsilon_\infty - \frac{\omega_D^2}{\omega(\omega - j\gamma_D)} - \frac{\Delta\varepsilon\Omega_L^2}{(\omega^2 - \omega_L^2) - j\Gamma_L\omega} \quad (1)$$

where $\varepsilon_\infty = 5.9673$ is the high frequency dielectric constant, $\Delta\varepsilon = 1.09$ is the weighted coefficient, ω is the guiding optical angular frequency, ω_D and γ_D are the plasmon frequency and the damping frequency, respectively. Ω_L is the oscillator strength of the Lorentz oscillator. Γ_L represents the frequency spectrum width of the Lorentz oscillator. The values of the parameters are: $\omega_D / 2\pi = 2113.6THz$, $\gamma_D / 2\pi = 15.92THz$, $\Omega_L / 2\pi = 650.7THz$, $\Gamma_L / 2\pi = 104.86THz$.

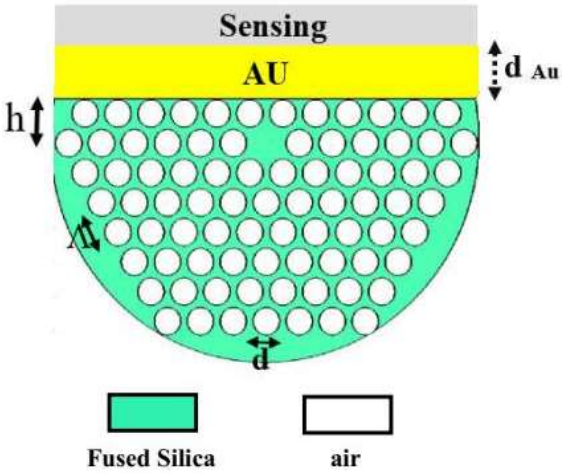

Fig. **1.** proposed D-Shaped SPR based PCF biosensor.

The leakage loss is an important parameter in designing of PCF with a finite number of air holes. Also, this leakage loss is known as the confinement loss. The confinement loss is eliminated provided the number of air holes in cladding is infinite. But, the number of air holes is finite in the practical PCF. Therefore, the power will leak transversely through the cladding, and the longitudinally propagating wave will be attenuated. The confinement loss depends on the core porosity and the number of air holes used in the cladding. Hence, to compute the confinement loss, a boundary condition is required, which produces no reflection at the boundary. A circular perfectly matched layers (PMLs) is required as the most efficient absorption boundary condition to calculate this loss. The confinement loss (L_{loss}) is given by:

$$L_{loss} = 8.686\frac{2\pi}{\lambda}\mathrm{Im}(n_{eff}) \times 10^4 \ (dB/cm) \quad (2)$$

where λ is the wavelength of incident light in micrometer, and $\mathrm{Im}(n_{eff})$ is the imaginary part of the effective refractive index. The effective

refractive index is defined by $n_{eff} = \beta / k_0$ where $k_0 = 2\pi / \lambda$ and β is the propagation constant. The effective refractive index has the real and the imaginary parts. The confinement loss is calculated from the imaginary part of n_{eff} . If the refraction index difference between the core and the cladding can be weaker by the central air hole, a significant confinement loss appears. Also, increasing of the number of hole layers in the cladding can reduce the confinement loss in PCFs. In this paper, we used different materials as a sensing layer. The refractive index of the samples as a sensing layer is shown in Table 1.

Table **1.** Refractive index of the sensing material

Name	Refractive index
Water	1.333
Blood Plasma	1.350
YD-10B	1.369
Hemoglobin	1.380

III. RESULT AND DISCUSSION

In Fig. 2, we plotted the confinement loss of the fundamental core mode and the dispersion curve of SPPs for structure with water as a sensing layer. According to Fig. 2, the strong SPR effect arises at 588 nm, where $\mathrm{Re}(n_{eff})$ of both modes coincide with each other and a intensive peak forms on the loss spectra. The confinement loss is dependent on the imaginary part of effective index ($\mathrm{Im}(n_{eff})$). At the specific wavelength (588 nm), the effective index of the fundamental core mode and the SPP mode are equal which leads to maximum energy transfer from fundamental core mode to SPP mode[13]. The field distribution of the fundamental mode in the proposed structure is plotted in Fig. 3.

Firstly, we consider the influence of the gold layer thickness to sensing performance. Therefore, the confinement loss spectra for the four different materials as a sensing layer (water, blood plasma, YD-10B, hemoglobin) with different refractive indexes in the range of 1.333 to 1.380 are plotted by variation of the gold layer thickness in the interval of 40 to 60 nm in Fig. 4.

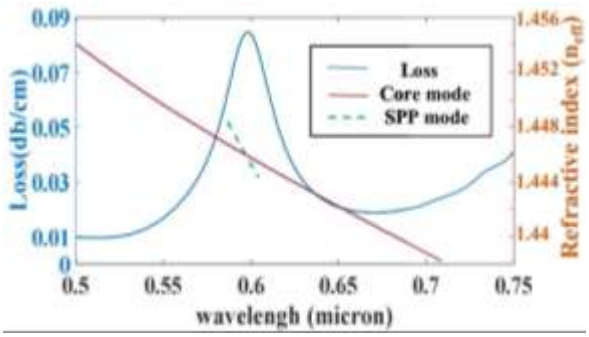

Fig. **2.** The confinement loss spectra of the fundamental core mode and the dispersion relation as function of the wavelength for structure with water as a sensing layer (n=1.333). The other parameters are $\Lambda = 1.9\mu m$, $\mathrm{d} = 1.4\mu m$, and $\mathrm{d}_{\mathrm{Au}} = 45nm$.

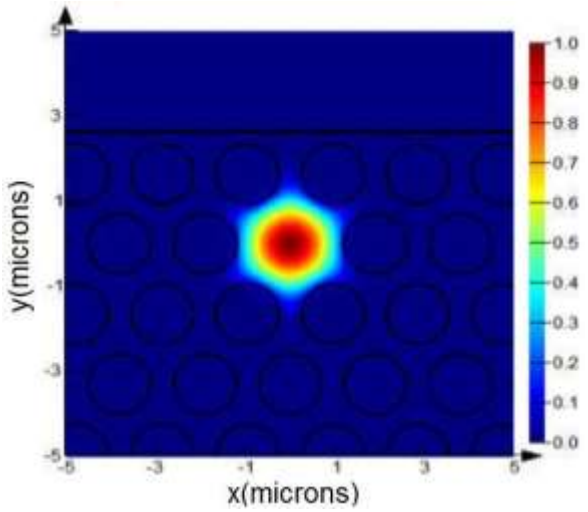

Fig. **3.** Fundamental mode distribution for structure with $\Lambda = 1.9\mu m$, $\mathrm{d} = 1.4\mu m$, and $\mathrm{d}_{\mathrm{Au}} = 45nm$.

According to Fig. 4, when the refractive index of the sensing layer increases (water to hemoglobin), the resonant wavelength shifts to longer wavelengths, and the maximum value of the confinement loss increases. In Fig. 4(a), the minimum value of the confinement loss is 0.0151 dB/cm at the wavelength of 574.4 nm. Also, the maximum value of the confinement loss is 0.0899 dB/cm at the wavelength of 647.1nm. Similar behavior is observed in Figs. 4(b) and 4(c) in the confinement loss spectra in terms of wavelength for studied refractive index range. Briefly, from the Figs 4(a) to 4(c), we observe that as the thickness of Au increases, the maximum value of the confinement loss decreases and the resonant wavelength shifts to longer wavelengths. Tables 2-4 show the variation of the maximum

value of the confinement loss for different sensing layers and the different thickness of Au layer.

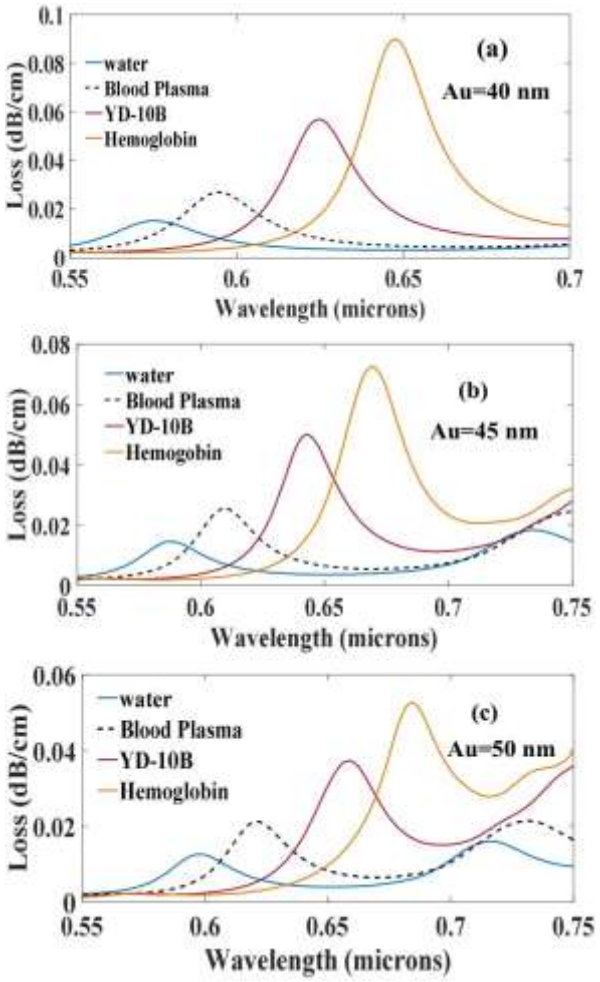

Fig. **4.** The confinement loss as function of wavelength for different sensing layers and different values of the gold layer thickness of d_{Au} = (a) 40nm, (b) 45nm, and (c) 50nm. The other parameters are $\Lambda = 2\mu m$, and $d = 1.6\mu m$.

Further, the confinement loss as a function of the wavelength for different value of the hole diameter, d is shown in Fig. 5. When the hole diameter value increases, the maximum value of the confinement loss decreases and the resonant wavelength shifts to the short wavelength.

In Fig. 5(a), the minimum value of the confinement loss is 0.2703dB/cm at the wavelength of 593.5 nm. Also, the maximum value of the confinement loss is 1.208 dB/cm at the wavelength of 689.4nm. Similar behavior is observed in Fig. 5(b). With comparison of data in Table **3**, Table **5** and Table **6,** it can be seen that when the diameter of the air hole set to 1.4 μm, the maximum resonant shift occurs about of 95nm.

Table **2.** Variation of the refractive index (RI), the resonant wavelength, and the confinement loss for different sensing layers with $\Lambda = 2\mu m$, $d = 1.6\mu m$, and $d_{Au} = 40nm$.

Molecular	RI	Wavelength (nm)	Loss (dB/cm)
Water	1.333	575.4	0.0151
Blood Plasma	1.350	594.5	0.0269
YD-10B	1.369	624.5	0.0569
Hemoglobin	1.380	647.1	0.0899

Table **3.** Variation of the refractive index (RI), the resonant wavelength, and the confinement loss for different sensing layers with $\Lambda = 2\mu m$, $d = 1.6\mu m$, and $d_{Au} = 45nm$.

Molecular	RI	Wavelength (nm)	Loss (dB/cm)
Water	1.333	587.7	0.0146
Blood Plasma	1.350	609.6	0.0255
YD-10B	1.369	642.4	0.0499
Hemoglobin	1.380	668.8	0.0725

Table **4.** Variation of the refractive index (RI), the resonant wavelength, and the confinement loss for different sensing layers with $\Lambda = 2\mu m$, $d = 1.6\mu m$, and $d_{Au} = 50nm$.

Molecular	RI	Wavelength (nm)	Loss (dB/cm)
Water	1.333	597.5	0.0125
Blood Plasma	1.350	621.3	0.0212
YD-10B	1.369	659	0.0372
Hemoglobin	1.380	684.1	0.0526

Table **5.** Variation of the refractive index (RI), the resonant wavelength, and the confinement loss for different sensing layers with $\Lambda = 2\mu m$, $d = 1.4\mu m$, and $d_{Au} = 45nm$.

Molecular	RI	Wavelength (nm)	Loss (dB/cm)
Water	1.333	593.5	0.2703
Blood Plasma	1.350	618.1	0.4432
YD-10B	1.369	657.7	0.8315
Hemoglobin	1.380	689.4	1.208

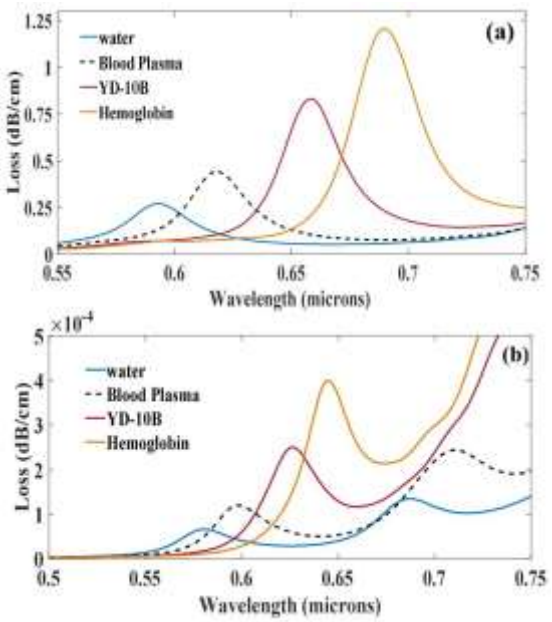

Fig. **5.** The confinement loss as a function of the wavelength for different sensing layers and different hole diameters d = **(a)** 1.4μm and **(b)** 1.8μm. The other parameters are $\Lambda = 2\mu m$, and $d_{Au} = 45nm$.

Table **6.** Variation of the refractive index (RI), the resonant wavelength, and the confinement loss for different sensing layers with $\Lambda = 2\mu m$, $d = 1.8\mu m$, and $d_{Au} = 45nm$.

Molecular	RI	Wavelength (nm)	Loss (dB/cm)
Water	1.333	580.01	0.66×10^{-4}
Blood Plasma	1.350	598.4	1.2×10^{-4}
YD-10B	1.369	626.74	2.5×10^{-4}
Hemoglobin	1.380	644.78	3.9×10^{-4}

Next, we plotted the confinement loss spectra for different pitch sizes from 1.9 to 2.1 μm with d=1.4 μm and the thickness of Au layer as 45 nm (Fig. 6). As illustrated in Fig. 6, with increasing of the pitch size, the maximum value of the confinement loss increases and the resonant wavelength shifts to the short wavelength. Also, according to Table 7 to Table 9, the maximum resonant shift is obtained about 119nm when the pitch size sets to 1.9 μm.

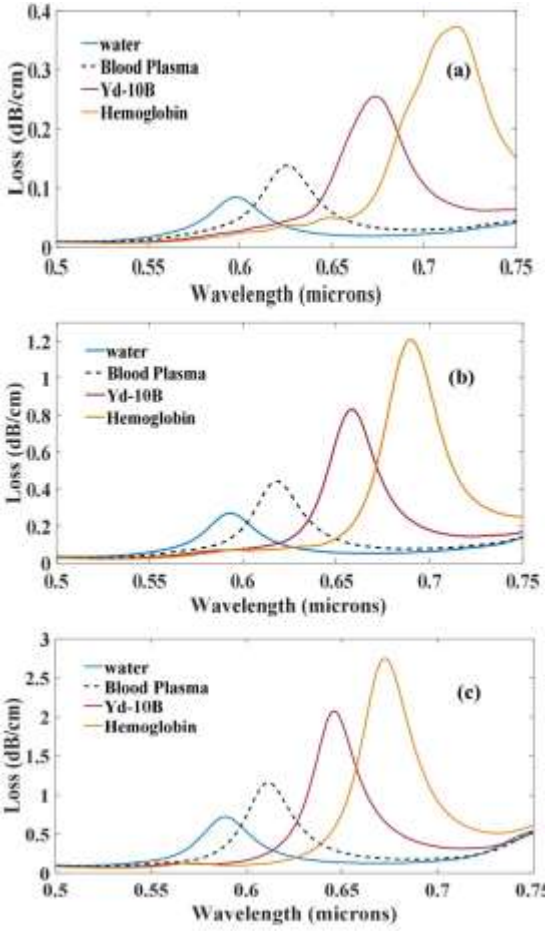

Fig. **6.** The confinement loss spectra with different sensing layers and different pitch sizes Λ= **(a)** 1.9 μm **(b)** 2 μm **(c)** 2.1 μm The other parameters are $d = 1.4\mu m$, and $d_{Au} = 45nm$.

Table **7.** Variation of the refractive index (RI), the resonant wavelength, and the confinement loss for different sensing layers with $\Lambda = 1.9\mu m$, $d = 1.4\mu m$, and $d_{Au} = 45nm$.

Molecular	RI	Wavelength (nm)	Loss (dB/cm)
Water	1.333	597.5	0.084
Blood Plasma	1.350	625.6	0.138
YD-10B	1.369	673.8	0.255
Hemoglobin	1.380	717	0.373

Table **8.** Variation of the refractive index (RI), the resonant wavelength, and the confinement loss for different sensing layers with $\Lambda = 2\mu m$, $d = 1.4\mu m$, and $d_{Au} = 45nm$.

Molecular	RI	Wavelength (nm)	Loss (dB/cm)
Water	1.333	593.4	0.27
Blood Plasma	1.350	618	0.443
YD-10B	1.369	658.9	0.830
Hemoglobin	1.380	689.3	1.21

Table **9.** Variation of the refractive index (RI), the resonant wavelength, and the confinement loss for different sensing layers with $\Lambda = 2.1\mu m$, $d = 1.4\mu m$, and $d_{Au} = 45nm$.

Molecular	RI	Wavelength (nm)	Loss (dB/cm)
Water	1.333	588.7	0.720
Blood Plasma	1.350	610.7	1.15
YD-10B	1.369	646.1	2.07
Hemoglobin	1.380	672.2	2.75

Now, we analyze the relative sensitivity by varying of the gold layer thickness and the other parameters of PCF biosensor such as, diameters of holes, d and pitch size, Λ. The RI sensitivity of biosensor, S, can be expressed as [8]:

$$S = \frac{\Delta\lambda_{peak}}{\Delta n_a};[nm/RIU] \quad (3)$$

Here, $\Delta\lambda_{peak}$ stands for the shift of the resonant wavelength and Δn_a the variation of the refractive index of sensing medium. The refractive index of resolution is defined as [9-12]:

$$R = \Delta n_a \frac{\Delta\lambda_{\min}}{\Delta\lambda_{peak}};[RIU] \quad (4)$$

Here, we considered $\Delta\lambda_{\min} = 0.1nm$. First, we consider the effect of thickness of Au layer to achievement of the high sensitivity for the proposed PCF biosensor. So we change the thickness of Au layer from 40 nm to 50 nm with step of 5nm to obtain the highest sensitivity. The highest sensitivity achieved with the thickness of Au layer as 45nm. The second important parameter in the sensitivity of PCF biosensors is the hole diameter (d). Therefore, the influence of the variation of d on the sensitivity of the biosensor is studied in Fig. 8. It shows the decrease of sensitivity when the hole diameter changes from 1.4 μm to 1.6 μm. So, the best value for the hole diameter of proposed PCF biosensor with the highest sensitivity is d=1.4 μm. Third, the value of the pitch size, Λ plays an important role in the enhancement of the relative sensitivity for the PCF biosensors. Hence, here we studied the sensitivity for proposed PCF biosensor by variation in the pitch size from 1.9 μm to 2.1 μm with $d_{Au} = 45nm$ and $d = 1.4\mu m$. As shown in Fig.9, the maximum sensitivity can be obtained when the pitch size set to be 1.9 μm.

Therefore, according to Fig.7 to Fig.9, the highest relative sensitivity of 2506 nm/RIU is obtained with the structural parameters of $\Lambda = 1.9\mu m$, $d = 1.4\mu m$, and $d_{Au} = 45nm$.

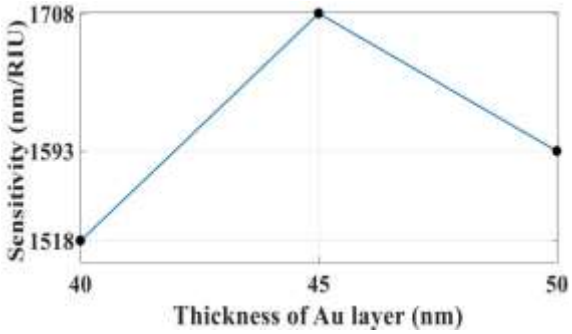

Fig. **7** Variation of the sensitivity in terms of the thickness of the Au layer with $\Lambda = 2\mu m$ and $d = 1.6\mu m$.

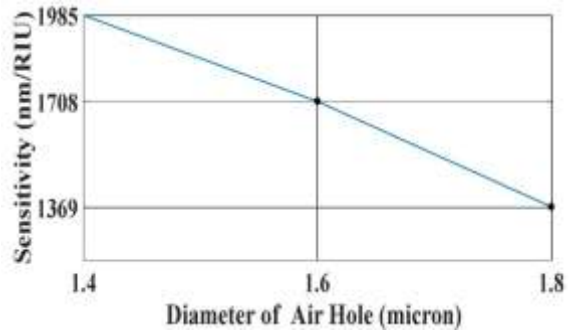

Fig. **8** Variation of the sensitivity in terms of the hole diameter with $\Lambda = 2\mu m$ and $d_{Au} = 45nm$.

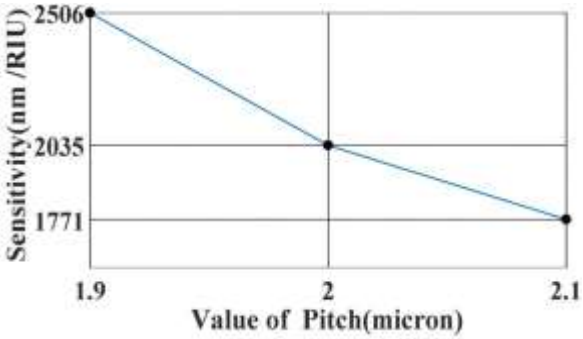

Fig. **9** Variation of the sensitivity in terms of the pitch size with $d_{Au} = 45nm$ and $d = 1.4\mu m$.

IV. CONCLUSION

In this paper, we proposed a D-shaped optical biosensor based on PCF. The relative sensitivity of 2506 nm per refractive index unit (nm/RIU) and the resolution of $1.25\times10^{-5}\,RIU$ is obtained with optimum structural parameters as $\Lambda=1.9\mu m,\ d=1.4\mu m,$ and $d_{Au}=45nm$. The simple design, small size and the high sensitivity makes it the excellent candidate to biosensing and the various applications with the refractive index range from 1.333 RIU to 1.38 RIU.

REFERENCES

[1] A. Olaru, C. Bala, N. Jaffrezic-Renault, and H. Y. Aboul-Enein, "Surface plasmon resonance (SPR) biosensors in pharmaceutical analysis," Crit. Rev. Anal. Chem. Vol. 45, pp. 97-105, 2015.

[2] S. Szunerits, N. Maalouli, E. Wijaya, J.P. Vilcot, and R. Boukherroub, "Recent advances in the development of graphene-based surface plasmon resonance (SPR) interfaces," Anal. Bioanal. Chem. Vol. 405, pp. 1435-1443, 2013.

[3] Y. Chen and H. Ming, "Review of surface plasmon resonance and localized surface plasmon resonance sensor," Photon. Sens. Vol. 2, pp. 37-49, 2012.

[4] N.A.S. Omar, Y.W. Fen, S. Saleviter, Y.M. Kamil, W.M.E.M.M. Daniyal, J. Abdullah, and M.A. Mahdi, "Experimental evaluation on surface plasmon resonance sensor performance based on sensitive hyperbranched polymer nanocomposite thin films," Sens. Actuator A-Phys. Vol. 303, pp. 111830 (1-10), 2020.

[5] S. Zhang, Y. Guo, T. Cheng, S. Li, and J. Li, "Surface plasmon resonance sensor based on a D-shaped photonic crystal fiber for high and low refractive index detection," Optik, Vol. 212, pp. 164697 (1-8), 2020.

[6] R. Alharbi, M. Irannejad, and M. Yavuz, "A short review on the role of the metal-graphene hybrid nanostructure in promoting the localized surface plasmon resonance sensor performance," Sensors, Vol. 19, pp. 862 (1-15), 2019.

[7] F. Wang, Z. Sun, C. Liu, T. Sun, and P.K. Chu, "A highly sensitive dual-core photonic crystal fiber based on a surface plasmon resonance biosensor with silver-graphene layer," Plasmonics, Vol. 12, pp. 1847-1853, 2017.

[8] H. Vahed and C. Nadri, "Sensitivity enhancement of SPR optical biosensor based on Graphene–MoS2 structure with nanocomposite layer," Opt. Mater. Vol. 88, pp. 161-166, 2019.

[9] X. Chen, L. Xia, and C. Li, "Surface plasmon resonance sensor based on a novel D-shaped photonic crystal fiber for low refractive index detection," IEEE Photon. J. Vol. 10, pp.1-9, 2018.

[10] S. Sen, M. Abdullah-Al-Shafi, and M.A. Kabir, "Hexagonal photonic crystal Fiber (H-PCF) based optical sensor with high relative sensitivity and low confinement loss for terahertz (THz) regime," Sensing and Bio-Sensing Research, Vol. 30, pp.100377 (1-9), 2020.

[11] G. An, S. Li, T. Cheng, X. Yan, X. Zhang, X. Zhou, and Z. Yuan, "Ultra-stable D-shaped optical fiber refractive index sensor with graphene-gold deposited platform," Plasmonics, Vol. 14, pp. 155-163, 2019.

[12] C. Liu, W. Su, Q. Liu, X. Lu, F. Wang, T. Sun, and P.K. Chu, "Symmetrical dual D-shape photonic crystal fibers for surface plasmon resonance sensing," Opt. express, Vol. 26, pp. 9039-9049, 2018.

[13] C. Liu, J. Wang, F. Wang, W. Su, L. Yang, J. Lv, G. Fu, X. Li, Q. Liu, T. Sun, and P.K. Chu, "Surface plasmon resonance (SPR) infrared sensor based on D-shape photonic crystal fibers with ITO coatings," Opt. Commun. Vol. 464, pp. 125496 (1-8), 2020.

[14] H. Ademgil and S. Haxha, "PCF based sensor with high sensitivity, high birefringence and low confinement losses for liquid analyte sensing applications," Sensors, Vol. 15, pp. 31833-31842, 2015.

[15] J.N. Dash and R. Jha, "Highly sensitive D shaped PCF sensor based on SPR for near IR," Optical and Quantum Electronics, Vol. 48, pp. 1403–1410, 2016.

[16] V. Kaur and S. Singh, "Design of D-Shaped PCF-SPR sensor with dual coating of ITO and ZnO conducting metal oxide," Optik, Vol. 220, pp. 165135 (1-16), 2020.

[17] M.S. Khan, K. Ahmed, M.N. Hossain, B.K. Paul, T.K. Nguyen, and V. Dhasarathan, "Exploring refractive index sensor using gold coated D-shaped photonic crystal fiber for biosensing applications," Optik, Vol. 202, pp.163649, 2020.

[18] M.N. Sakib, M.B. Hossain, K.F. Al-tabatabaie, I.M. Mehedi, M.T. Hasan, M.A. Hossain, and I.S. Amiri, "High performance dual core D-shape PCF-SPR sensor modeling employing gold coat," Results in Physics, Vol. 15, pp.102788 (1-18), 2019.

[19] H. Thenmozhi, M.M. Rajan, and K. Ahmed, "D-shaped PCF sensor based on SPR for the detection of carcinogenic agents in food and cosmetics," Optik, Vol. 180, pp. 264-270, 2019.

[20] S. Singh and Y.K. Prajapati, "Highly sensitive refractive index sensor based on D-shaped PCF with gold-graphene layers on the polished surface," Appl. Phys. A, Vol. 125, pp. 1-7, 2019.

[21] W. Zeng, Q. Wang and L. Xu, "Plasmonic refractive index sensor based on D-shaped photonic crystal fiber for wider range of refractive index detection," Optik, Vol. 223, pp. 165463 (1-9), 2020.

[22] M.B. Hossain, M.S. Hossain, S.R. Islam, M.N. Sakib, K.Z. Islam, M.A. Hossain, M.S. Hossain, A.S. Hosen, and G.H. Cho, "Numerical development of high performance quasi D-shape PCF-SPR biosensor: An external sensing approach employing gold," Results Phys. Vol. 18, pp. 103281 (1-21), 2020.

Mir Vahid Kazempour was born in Tabriz, Iran, in 1994. He received the B.Sc. degree in power engineering from the Islamic Azad University of Tabriz, Tabriz, Iran, in 2017 and the M.Sc. degree in Nanoelectronics engineering from the University of Tabriz, Tabriz, in 2020. His research interests are photonic crystal fiber, and application of plasmonics in sensors.

Hamid Vahed was born in Tabriz, Iran on July 11, 1982. He received Ph.D. degree in laser physics from the University of Tabriz, Tabriz, Iran in 2012. He is currently an associate professor with Faculty of Electrical and Computer Engineeing of the University of Tabriz, Tabriz, Iran. His research has focused on the study of switching and plasmonic devices.